ELSEVIER

Polymer 44 (2003) 2509–2518

polymer

www.elsevier.com/locate/polymer

Time-resolved X-ray scattering and calorimetric studies on the crystallization behaviors of poly(ethylene terephthalate) (PET) and its copolymers containing isophthalate units

B. Lee[a], T.J. Shin[a], S.W. Lee[a], J. Yoon[a], J. Kim[b], H.S. Youn[b], M. Ree[a,b,*]

[a]*Department of Chemistry, Center for Integrated Molecular Systems, Polymer Research Institute, BK21 Program, and Division of Molecular and Life Sciences, Pohang University of Science and Technology, San 31, Hyoja-dong, Nam-gu, Pohang 790-784, Republic of Korea*

[b]*Pohang Accelerator Laboratory, Pohang University of Science and Technology, San 31, Hyoja-dong, Nam-gu, Pohang 790-784, Republic of Korea*

Received 24 September 2002; received in revised form 25 December 2002; accepted 22 January 2003

Abstract

Time-resolved small-angle X-ray scattering (SAXS) measurements were carried out for PET and its copolymers undergoing isothermal crystallization. Wide-angle X-ray diffraction and differential scanning calorimetric measurements were also performed. Our data analysis of the SAXS results for PET and the copolymers clearly demonstrate that the one layer thickness l_1 (derived directly from the correlation functions of the measured SAXS profiles) is the lamellar crystal thickness d_c, not the amorphous layer thickness d_a. The observed d_c values are found to be always smaller than d_a, regardless of polymer composition. d_c is highly dependent on the crystallization temperature, showing that the degree of supercooling is the major factor determining the thickness of lamellar crystals. No thickening, however, occurs in isothermal crystallizations. The kinked isophthalate units in the copolymer are found to be mostly excluded from the lamellar crystals during the crystallization process, leading to an increase of the amorphous layer thickness. Moreover, the kinked, rigid nature of the isophthalate unit was found to restrict crystal growth along the chain axis of the copolymers and also to lower their crystallinity. Unlike d_c, d_a decreases with crystallization time, causing a reduction of the long period in the lamellar stack. This drop in d_a is interpreted in this paper by taking into account several factors that could influence crystallization behavior: the d_a distribution in the lamellar stacks and its variation with time, the number of lamellae in the lamellar stacks and their effect on the SAXS profile, and the relaxation of polymer chains in the amorphous layers.

Keywords: X-ray scattering; Calorimetry; Crystallization of PET and copolyesters

1. Introduction

The physical properties of a polymer depend primarily on its morphological structure. However, the morphological structures of polymers are generally very complicated, because of their long chain lengths and many possible conformations. The morphological structure is thus sensitive to the conditions under which the polymer is processed, for example the quenching regime used in its crystallization. The ultimate properties of a polymeric system, therefore, correlate directly with the manner in which it is processed. The relationship between processing conditions, morphological structure and polymer properties has been extensively studied over the past few decades.

Research into semi-crystalline polymers has utilized their crystallization behavior as the key to understanding their morphological structures. A typical semi-crystalline polymer is poly(ethylene terephthalate) (PET), which is widely used as an engineering plastic material. The crystallization of PET has been extensively investigated by various analytical techniques [1–17]. In particular, the small-angle X-ray scattering (SAXS) method has been widely employed to investigate the morphological structure of PET crystallized from melt [1,8–10,18–31]. It was concluded from these SAXS studies that the long period always decreases with increasing crystallization time [1,8–10,18–31]. Similar SAXS results have been reported for poly(ether ether ketone)s [1,19–25] and poly(aryl ether

* Corresponding author. Address: Department of Chemistry, Center for Integrated Molecular Systems, BK21 Functional Polymer Thin Group, Pohang University of Science and Technology, San 31, Hyoja-dong, Nam-gu, Pohang 790-784, Republic of Korea. Tel.: +82-54-279-2120; fax: +82-54-279-3399.

E-mail address: ree@postech.edu (M. Ree).

0032-3861/03/$ - see front matter © 2003 Elsevier Science Ltd. All rights reserved.
doi:10.1016/S0032-3861(03)00130-7

ether ketone)s [26]. These SAXS results are quite different from those observed for other common semi-crystalline polymers such as polyethylene, which undergo lamella thickening [32,33]. Much research effort has been put into explaining these differences, resulting in the proposal of several models of morphological structure that have been widely debated [1,8–10,18–25,27–31]. The conflicts between these models have mainly arisen over different interpretations of the correlation functions calculated from the observed SAXS patterns. More research into the data analysis of SAXS studies of the crystallization of PET is needed in order to determine the morphological parameters correctly.

Unlike PET, poly(ethylene isophthalate-*co*-terephthalate) (PEIT), which is a copolymer based on PET, has been rarely studied [7,15–17]. Hachiboshi et al. [7] investigated the crystallization of PEIT fiber specimens using SAXS and proposed that kinked isophthalate (IPT) units include into the lamellar crystals. However, they studied the crystallization of fiber-formed PEIT specimens rather than the crystallization of PEIT from melt. In fact, in the fiber formation process the polymer chains are preferentially aligned along the fiber drawing direction, moving favorably into lateral ordering, so kinked IPT units are more likely to be included into the resultant crystals. Such molecular crystallization in drawn fibers may be significantly different from crystallization from melt. The question remains whether kinked IPT units in PEIT include into or exclude from crystals formed by crystallization from melt.

To address the main two questions outlined above, in the present work we synthesized PET and PEIT copolymers containing 4.9–9.8 mol% IPT units and studied their crystallization. We conducted time-resolved SAXS measurements during the isothermal crystallization of PET samples and extended this procedure to the isothermal crystallization of PEIT copolymers. In addition, wide-angle X-ray diffraction (WAXD) and differential scanning calorimetry (DSC) measurements were performed on these samples.

2. Experimental

2.1. Polymerization and sample preparation

PET was synthesized from ethylene glycol and dimethyl terephthalate by bulk polycondensation, as described elsewhere [15–17]. Using the same synthetic method, poly(ethylene isophthalate-*co*-terephthalate) copolymers with various compositions were prepared from ethylene glycol, dimethyl terephthalate, and dimethyl isophthalate (see Fig. 1) [7]. From the PET homopolymer and its copolymers, three samples rich in ethylene terephthalate units were chosen for study. These samples, referred to as PET, 5IPT, and 10IPT, have the following characteristics. The isophthalate unit content was determined by proton nuclear magnetic resonance spectroscopy to be 4.9 mol% for 5IPT and 9.8 mol% for 10IPT. The molecular weight $\bar{M}_W$ was determined by viscometry [7] to be 36,000 for PET, 37,000 for 5IPT, and 36,000 for 10IPT. The polymers were melt-molded under compression in a nitrogen atmosphere and cooled to room temperature, producing 2-mm thick sheets. These polymer sheets were cut either into disks of diameter 4 mm for use in X-ray scattering measurements, or into tiny pieces for use in DSC measurements.

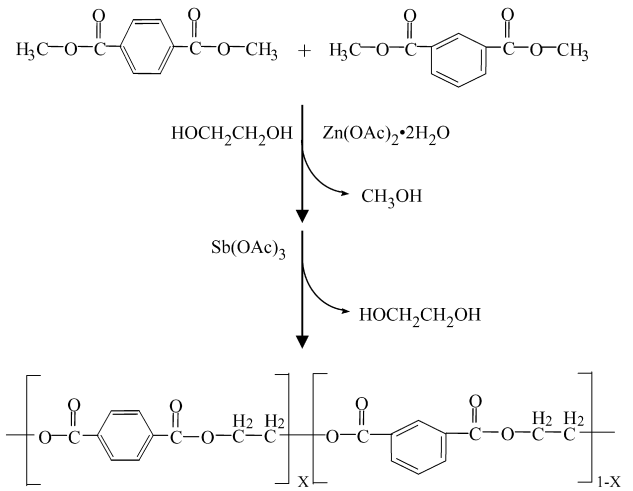

Fig. 1. Synthetic scheme and chemical structure of poly(ethylene isophthalate-*co*-terephthalate)s.

2.2. Time-resolved SAXS measurements and data analysis

SAXS measurements were conducted at the 4C1 beamline (BL) of the Pohang Light Source (PLS) facility with 2.5 GeV power at the Pohang University of Science and Technology. X-ray beams from a bending magnet of the PLS storage ring were focused by a toroidal silicon mirror coated with platinum [34,35]. The 4C1 BL was equipped with a W/B_4C double multiplayer monochromator [35]. The wavelength and size of the monochromatized X-ray beam were 1.608 Å and 0.6 × 0.6 mm, respectively. SAXS patterns were measured using a 1-dimensional silicon-photodiode array detector (Model X/PDA-2048, Princeton Instruments) consisting of 2048 pixels. A jumping hot-stage consisting of two independent chambers was employed. Each specimen was first melted for 5 min in the top chamber and then quickly jumped to the bottom chamber, which was held at the chosen crystallization temperature (T_c). The PET, 5IPT and 10IPT specimens were melted at 285, 275 and 265 °C, respectively. The temperature of each chamber was controlled by a Eurotherm controller with a K-type thermocouple. The specimen chambers had N_2 blowing-holes to protect the polymer samples from thermal oxidation at high temperatures. To correctly monitor the sample temperature, a third Eurotherm controller was used that had a K-type thin-wire thermocouple in direct contact with the specimen. The distance between sample and detector was

1.0 m. Scattering angle was calibrated with a collagen standard prepared from chicken tendon. SAXS measurements were carried out during isothermal crystallization of the polymer samples at various temperatures in the range 170–240 °C, and the final crystallized samples were immediately quenched to ice water temperature for the WAXD and DSC measurements. Each measurement was collected for 10 s, with an average count per pixel of about 1200. Each SAXS intensity profile was normalized to the incident X-ray beam intensity (monitored by an ionization chamber placed in front of the sample), and corrected further using a background run. Representative SAXS intensity profiles measured during crystallization at 230 and 216 °C are shown in Fig. 2a and b, respectively.

The measured SAXS intensity profiles were Lorentz-corrected as follows. Each measured SAXS profile was non-linear-least-square fitted with Porod's law [36,37]:

$$\lim_{q\to\infty} I(q) = I_b + \frac{K_p}{q^4} e^{-\sigma^2 q^2} \quad (1)$$

where $I(q)$ is the scattered intensity profile, I_b the constant scattering from density fluctuations, σ is related to the interfacial thickness between the lamellar crystal and amorphous layer, and K_p is the Porod constant. q is given by $q = (4\pi/\lambda)\sin\theta$, where λ is the wavelength of the X-ray source and 2θ is the scattering angle. The SAXS profile was then extrapolated to $q = 4\ \mathrm{nm}^{-1}$, corrected by subtraction of the value determined for I_b and then by multiplying by q^2, giving the Lorentz-corrected SAXS profile.

The corrected SAXS profile was then inverse-cosine-Fourier-transformed to a one-dimensional correlation function $\gamma_1(z)$ [38–40]:

$$\gamma_1(z) = \int_0^\infty q^2 I(q)\cos(qz)\mathrm{d}q \quad (2)$$

where z is the axis normal to the layer faces in the stack. The correlation function analysis can provide several morphological parameters, namely the long period L as well as the one layer thickness l_1 (either the lamellar crystal layer thickness d_c or the amorphous layer thickness d_a) according to Babinet's reciprocity.

2.3. WAXD measurements

WAXD measurements were carried out at room temperature in transmission mode on the samples quenched to ice water temperature after the isothermal SAXS measurements had been completed. WAXD was performed using a Rigaku vertical diffractometer (Model RINT-2500) with a rotating anode X-ray generator and a Ni filter. The Cu Kα radiation source was operated at 4 kW. A divergence slit of 0.5° was employed, together with a scattering slit of 0.5° and a receiving slit of 0.15 mm. All measurements were carried out in the $\theta/2\theta$ mode. The 2θ scan data were collected at 0.02° intervals over the range 3–60° with a scan speed of 0.1°(2θ)/min. The diffraction peaks in each WAXD pattern were separated and fitted with Voight functions on a single baseline using a peak-fitting program (Peakfit, Jandel

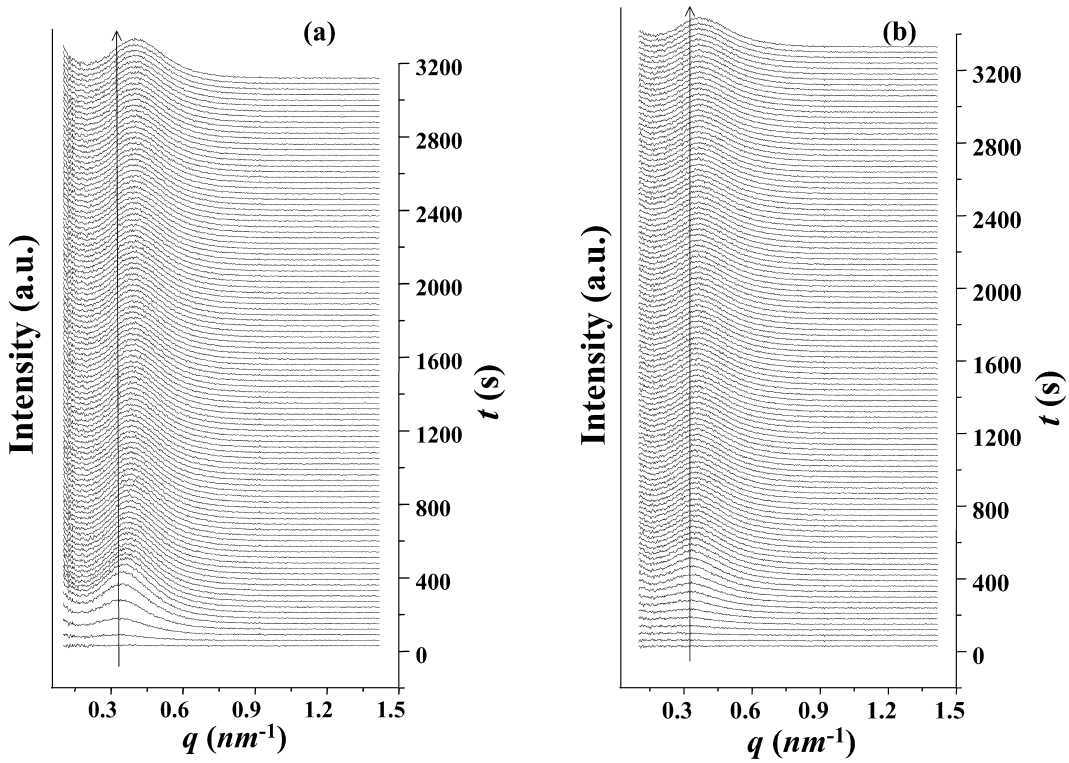

Fig. 2. (a) Time-resolved SAXS patterns of PET polymer measured during isothermal crystallization at 230 °C for 60 min. (b) Time-resolved SAXS patterns of 5IPT copolymer measured during isothermal crystallization at 216 °C for 60 min.

Scientific). The coherence length (i.e. mean crystallite dimension perpendicular to a given diffraction plane) of the separated diffraction peaks was estimated using the Scherrer equation [41,42].

2.4. DSC measurements

DSC measurements were carried out as follows. One series of measurements were carried out for the samples quenched to ice water temperature after isothermal SAXS measurements had been completed at the chosen values of T_c. A heating rate of 3.0 °C/min was employed. The other series of measurements were performed during isothermal crystallization of the polymer samples at various temperatures in the range 170–240 °C for 60 min and then continued during subsequent re-melting of the crystallized samples with a heating rate of 3.0 °C/min. All measurements were conducted in a nitrogen atmosphere using a Seiko calorimeter calibrated with indium and tin standards.

3. Results and discussion

3.1. SAXS analysis

PET, 5IPT and 10IPT have been previously determined to have equilibrium melting temperatures T_m^0 of 275.4, 266.5 and 261.9 °C, respectively [15–17]. In addition, both copolymers have been determined to be random copolymers [15–17]. For PET, 5IPT and 10IPT, time-resolved SAXS measurements were conducted during their isothermal crystallizations from the melt over a temperature range of 170–240 °C. Fig. 2 shows typical SAXS patterns for PET and 5IPT polymers undergoing isothermal crystallization at the chosen temperatures. In all cases, no SAXS pattern is detected initially, but develops with the structural evolution associated with crystallization. With increasing crystallization time the SAXS peak increases in intensity and its maximum shifts to the high q region, finally remaining unchanged with further increase of the crystallization time.

Fig. 3 shows a typical correlation function $\gamma_1(z)$ obtained from the Lorentz-corrected SAXS intensity profile of a PET sample crystallized at 210 °C. As shown in the figure, the one layer thickness l_1 in the lamellar crystal and amorphous layer stack is estimated from the linear fit of the first decay slope in the plot of $\gamma_1(z)/\gamma_1(0)$ versus z, according to the correlation function analysis described elsewhere [38–40]. The long period L is obtained from the first peak maximum (z_{max}) of the same plot; the other layer thickness l_2 ($= L - l_1$) can be obtained from L and l_1. This correlation function analysis was extended to all measured SAXS intensity profiles after Lorentz correction, providing l_1 and L databases. In the present study, l_1 was found to be always shorter than l_2, regardless of polymer composition. l_1 can be assigned to either the lamellar crystal thickness or to the amorphous layer thickness of the lamellar stacks formed in the polymer samples, according to Babinet's reciprocity. In the present study l_1 is larger for PET than for the copolymers crystallized at the same degree of supercooling ΔT ($= T_m^0 - T_c$). On the other hand, the value of l_2 is smaller for PET than for the copolymers. In the present study as well as in our previous DSC results [15–17], PET exhibits a higher crystal melting temperature than the copolymers when they are crystallized at the same degree of supercooling, indicating that the lamellar crystals formed in the PET sample are thicker and more perfect than those formed in the copolymer samples. Based on the combined results of the correlation function analysis and of the DSC measurements, we clearly assign the value determined for l_1 as corresponding to the lamellar crystal layer thickness d_c and l_2 as corresponding to the amorphous layer thickness d_a. These layer thickness assignments are in contradiction to those derived from previous SAXS analyses of PET [8,31,43–45].

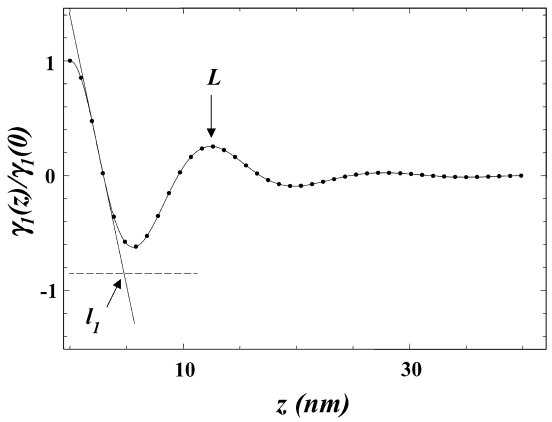

Fig. 3. Correlation function $\gamma(z)$ obtained from the SAXS intensity profile of PET homopolymer crystallized at 210 °C: L is the long period; l_1 is the one layer thickness of the lamellar and amorphous layer stack. z is the axis normal to the plane of a lamellar stack.

Fig. 4 shows the time dependence of the morphological parameters (the long period L, the amorphous layer thickness d_a and the lamellar crystal thickness d_c) obtained from the correlation function analysis of the SAXS patterns measured during isothermal crystallization of the PET homopolymer and of the 5IPT copolymer at various temperatures. As shown in the figure, for both PET and its copolymer the long period L was found to decrease during isothermal crystallization over the temperature range considered. A similar trend was observed in the L variation measured for the crystallization of the 10IPT copolymer. Moreover, similar trends in L have been reported previously for the crystallization of PET [8,31,43–45].

Unlike the long period, the lamellar crystal thickness d_c varies very little with time during the crystallization of PET, indicating that no thickening occurs during the isothermal crystallization [see Fig. 4(a)). A similar trend is observed for the crystallization of the copolymers, as shown in Fig. 4(b) for 5IPT.

Furthermore, d_c varies little with the isophthalate unit

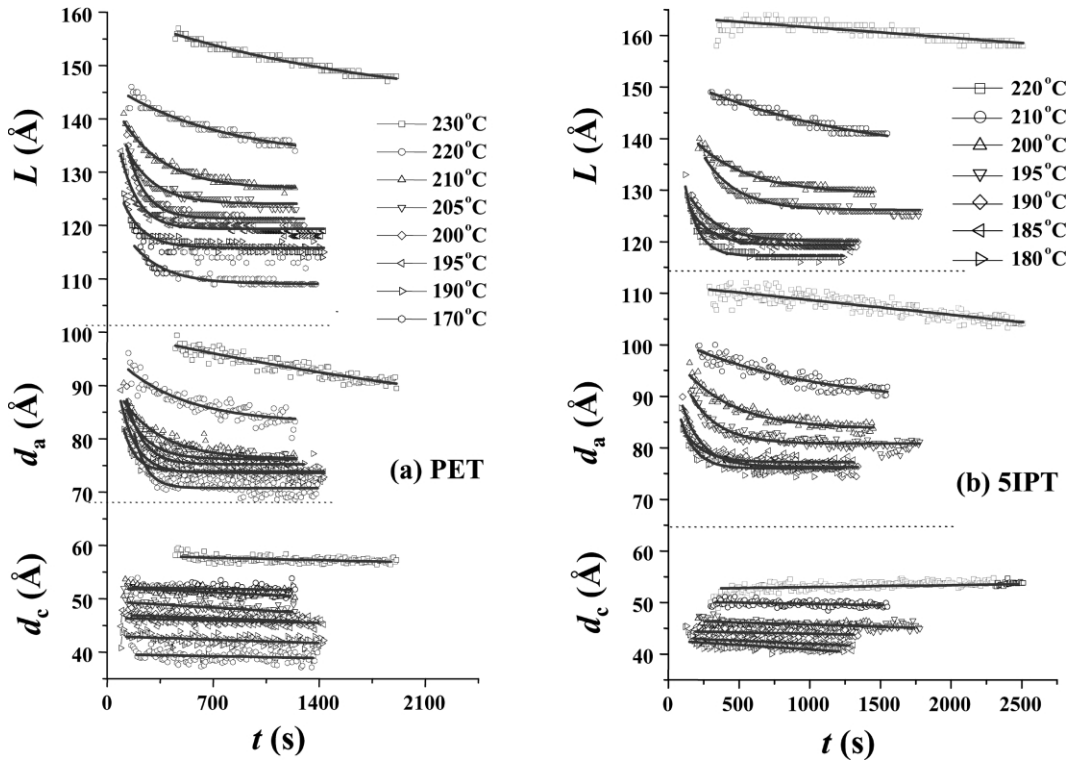

Fig. 4. Variation of morphological parameters (the long period L, the amorphous layer thickness d_a, and the lamellar crystal thickness d_c) with time, obtained from the time-resolved SAXS patterns obtained during isothermal crystallization at various temperatures: (a) PET homopolymer; (b) 5IPT copolymer.

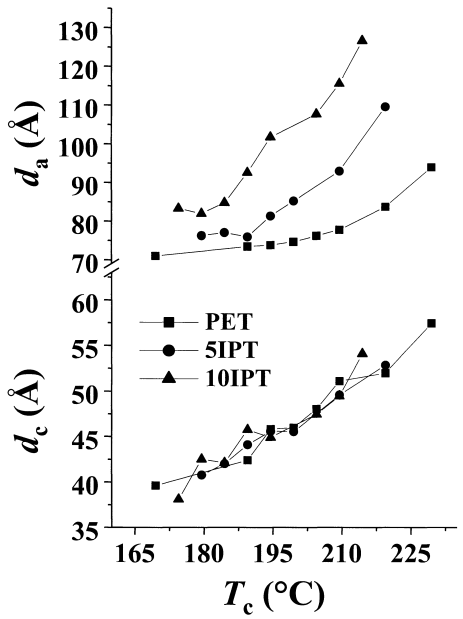

Fig. 5. Variations of amorphous layer thickness d_a and lamellar crystal thickness d_c with crystallization temperature in PET polymer and its copolymers (5IPT and 10IPT). For each polymer, the morphological parameters were obtained from the SAXS pattern measured at $t = (t_{Q_{max}} + 100\ \text{s})$, where $t_{Q_{max}}$ is the time at which the invariant Q of the SAXS pattern reaches its maximum during crystallization.

content of PET and its copolymers crystallized at the same temperature, as shown in Fig. 5. Here, the d_c and d_a variations were measured for PET and its copolymers (5IPT and 10IPT) crystallized at the chosen values of T_c for the time ($t_{Q_{max}}$) required for the invariant Q to reach a maximum (see Fig. 8; the invariant Q is discussed in a later section). d_c exhibits values in the range 38–58 Å, depending on T_c. These d_c values correspond to the dimensions of 4 to 6 ethylene terephthalate units in an extended chain. For the 5IPT and 10IPT copolymers which have $\bar{M}_W = 36,000–37,000$, adjacent isophthalate units are on average separated by 26 to 38 ethylene terephthalate units. This interdistance on the copolymer chain is sufficient to form lamellar crystals with $d_c = 38–58$ Å, excluding kinked isophthalate units. One might imagine that kinked isophthalate units are included in crystal formation in the early stages of crystallization and then excluded from the crystal at a later stage. If this were the case, the exclusion process would cause an increase in the density of the lamellar crystal and a decrease in the density of the amorphous layer, leading to a large density difference between these layers. This density difference should cause an increase in the SAXS intensity profile and in the invariant in the later stages of crystallization. However, the SAXS results produced in this study show no such behavior. We therefore conclude that during the crystallization lamellar crystals form and grow laterally without thickening, and that isophthalate units are mostly excluded during this process.

Similar results have been reported for poly(ethylene-*co*-oxydiethylene terephthalate) by Fakirov and coworkers [11–14]. They also conclude that the oxydiethylene terephthalate units are excluded from the lamellar crystals formed during crystallization. However, they estimated the crystal thickness d_c incorrectly, taking the value of d_c to be the product of the long period L with the bulk volume crystallinity x_c rather than with the relative volume fraction of lamellae φ_c.

The question still remains as to why the homopolymer and the copolymers form lamellar crystals with almost the same value of d_c when crystallized at the same crystallization temperature. Note that the copolymers have lower T_m^0 than the PET homopolymer [15–17]. Thus, if only the degree of supercooling is taken into account, one might expect the copolymers to produce thicker lamellar crystals than the homopolymer. However, this behavior was not observed. Instead, as is described in Section 3.2, the measured WAXD patterns indicate that growth along the chain direction is very restricted compared to growth along the lateral direction. It is likely that growing lateral planes of lamellae have a chance to grasp the sequence composed of crystallizable unit, but this situation does not apply in the chain direction because the randomly distributed kinked and relatively rigid isophthalate units restrict ordering.

In contrast, as shown in Fig. 5, d_a increases with increasing isophthalate unit content, even though the samples with different isophthalate unit content crystallize at the same temperature. In addition, the difference between the d_a values of PET and of its copolymers becomes large at higher isothermal crystallization temperatures. The increase in the thickness of the amorphous layers leads to a reduction in the crystallinity; in fact, the reduction of overall crystallinity in the PET due to the incorporated IPT units is evident in the DSC results reported previously [15–17]. This increase of d_a in the copolymer may be due to the exclusion of kinked isophthalate units from the lamellar crystals into the amorphous region.

Furthermore, d_a decreases with time during isothermal crystallization, regardless of polymer composition, as seen in Fig. 4. d_a decreases more rapidly with time in the PET homopolymer than in the copolymers for systems crystallizing at the same degree of supercooling. There are two major factors that could account for the decrease in d_a during crystallization. The first possible factor is the distribution of the values of d_a and its variation with time. The number of lamellae increases with time during stack building, which reduces the standard deviation in the value of d_a and narrows its distribution. This has the effect of shifting the peak maximum of the SAXS profile into the high q region, as has been pointed out by Vignaud and Schultz [46]. The second possible factor is the relaxation of the polymer chains in the amorphous layers. When the lamellar stacks form, the polymer chains in the amorphous layers may be in a strained state. These strained polymer chains relax with time, leading to a reduction in d_a. These considerations collectively lead to the conclusion that the decrease of the long period L during crystallization should be attributed to the reduction of the amorphous layer thickness d_a with crystallization time.

3.2. WAXD analysis

WAXD measurements were performed on samples quenched to ice water temperature after isothermal crystallization at 220 °C for 60 min. The measured WAXD patterns are shown in Fig. 6a.

It has been previously reported that the volume of the crystal lattice unit cell is 212.5 Å^3 for the crystals of PET homopolymer and 288.4 Å^3 for those of poly(ethylene isophthalate) (PEI) homopolymer [6,7]. If the kinked isophthalate units in the copolymers were cocrystallized with terephthalate units, the copolymer lamellar crystal would be expected to have a lower density than the PET lamellar crystal. Such a change in the crystal density would cause a shift in the X-ray diffraction peaks to either the low- or high-angle region, depending on the number of cocrystallized isophthalate units. The change in the crystal lattice constant (which directly relates to the shift of the diffraction peak) due to the incorporation of kinked IPT units can be estimated by the following equation:

$$a = f_{PEI}a_{PEI} + (1 - f_{PEI})a_{PET} \quad (3)$$

where a is the lattice constant of the cocrystal, a_{PEI} ($= 5.20$ Å) is the lattice constant of the PEI crystal [7], a_{PET} ($= 4.56$ Å) is the lattice constant of the PET crystal [6], and f is the fraction of IPT units in the PET crystal lattice.

For example, the formation of cocrystal containing 5 mol% IPT units would cause a shift in the (100) diffraction peak of around 0.2° toward the low angle region. However, as seen in Fig. 6a, such a shift of the diffraction peak is not detected for either the 5IPT or 10IPT copolymer samples. Rather, the positions of all diffraction peaks in the copolymers match those in the PET homopolymer, indicating there are no peak shifts in the copolymers. These results collectively indicate that the densities of the crystal lattice units in the copolymers are nearly the same as the density of these units in PET. This result might be attributed to the crystallization process of the copolymers, whose kinked isophthalate units are unlikely to include into the lamellar crystals.

The PEIT copolymers investigated in the present study contain only 4.9 and 9.8 mol% IPT units, respectively, as a minor component. Thus, it might be assumed that kinked IPT units in the copolymer include into the lamellar crystals as simple defects at a relatively low level, rather than as cocrystal components, causing the broadening of diffraction peaks without any substantial shift in their position. As seen in Fig. 6a, such a peak broadening is not detected in the diffraction peaks of the 5IPT and 10IPT copolymers. It is found instead that the full width at half maximum (FWHM)

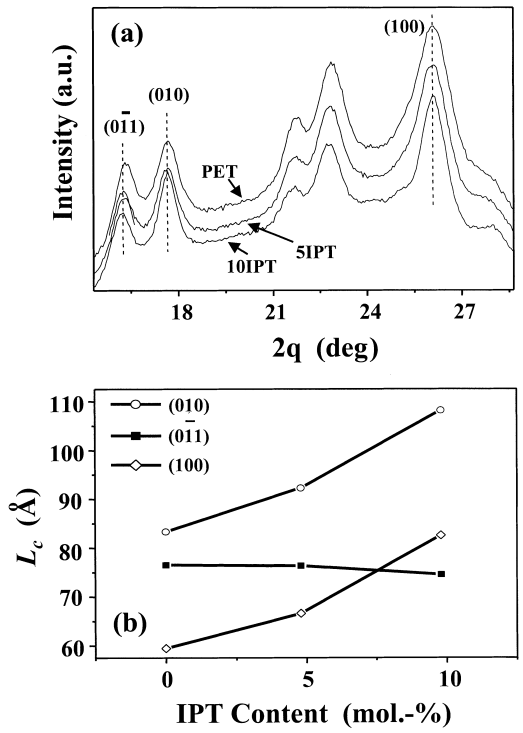

Fig. 6. (a) WAXD patterns for the samples quenched after isothermal crystallization at 220 °C for 60 min. (b) Coherence lengths determined from the diffraction peaks in (a).

of each diffraction peak of the copolymers is comparable to or narrower than that of the corresponding diffraction peak of PET.

The WAXD peaks in Fig. 6a were further analyzed to obtain structural information about the lamellar crystal dimension (i.e. the coherence length) in the direction normal to the individual diffraction plane. The coherence length L_c of a diffraction plane was determined from the full width at half peak maximum by using the Scherrer formula. The estimated values of L_c are plotted together in Fig. 6b as a function of polymer composition. As seen in Fig. 6b, $L_{c(010)}$ [i.e. the coherence length of the (010) diffraction plane] increases as the IPT content in the polymer increases. A similar trend is observed for the variation of $L_{c(100)}$ with polymer composition. We presume that the estimated value for L_c can be mainly attributed to the lamellar crystal size along the direction normal to the chosen diffraction plane. With this assumption, these results indicate that the lamellar crystal size in the lateral directions (x- and y-axis) is the largest for the lamellar crystals of the 10IPT copolymer, intermediate for those of 5IPT, and smallest for those of PET. Such formation of larger crystals in the copolymers might be attributed to their lesser degree of supercooling compared to that of the PET sample. At lower degrees of supercooling, the copolymer chains have more mobility and indeed undergo crystal growth more favorably, although their crystallization rates are slower. $L_{c(100)}$ and $L_{c(010)}$ give information on the lamellar crystal dimensions in the lateral x- and y-directions, respectively, whereas $L_{c(0\bar{1}1)}$ provides information on the lamellar crystal thickness. Unlike the $L_{c(100)}$ and $L_{c(010)}$ variations, $L_{c(0\bar{1}1)}$ decreases very little with increasing polymer IPT content, as seen in Fig. 6b. One might expect that the copolymers would produce thicker lamellar crystals due to their lesser degree of supercooling, because the crystallization of a polymer is generally primarily controlled by the degree of supercooling. However, our result is contrary to this expectation. The observed result might be due to significant restriction of crystal growth along the direction of lamellar crystal thickness (i.e. the chain axis) by IPT units in the copolymers. More specifically, crystal growth along the chain axis in the copolymer is restricted by kinked IPT units in the copolymer that were excluded from the lamellar crystals formed during crystallization. If IPT units in the copolymers are included in the lamellar crystals as defects, their fraction may be very small.

3.3. DSC and SAXS invariant Q analysis

Fig. 7 shows typical DSC thermograms obtained from the re-melting of samples of PET and its copolymers after crystallization for 60 min at the chosen temperatures. Both PET and its copolymers reveal more than one melting peak, regardless of the crystallization conditions. Such multiple melting behavior has been frequently reported for PET [2,3,8–10,15–17]. As shown in Fig. 7, the PET sample crystallized at 230 °C reveals two melting peaks: one strong peak in the high temperature region with a very large heat of melting, and another weak peak in the low temperature region. In general, lamellar crystals formed by primary crystallization are larger than those formed by secondary crystallization, causing them to melt in the high temperature region. Thus, the peak in the high temperature region can be assigned to the melting of crystals formed by primary crystallization while the peak in the low temperature region is assigned to the melting of the crystals formed by secondary crystallization. Similar melting behavior is observed for the 5IPT and 10IPT samples crystallized at 208 °C, as seen in Fig. 7.

Bulk volume crystallinities (x_c) of PET and its copolyesters were determined from the heats of fusion (ΔH_f) obtained from the melting endotherms in the DSC measurements, using the ΔH_f of the fully crystallized PET homopolymer (117.6 J/g) [15–17,47]. The determined values of x_c relate directly to the invariant Qs of the SAXS intensity profiles measured from the crystallized samples as well as to the difference between the electron densities of the crystalline and non-crystalline regions ($\rho_c - \rho_a$) [8,22,24,36–40,48]:

$$Q = x_c(1 - x_c)(\rho_c - \rho_a)^2 \quad (4)$$

Eq. (4) was derived under the assumption that the samples have ideally sharp interfaces between the crystalline and non-crystalline phases and that the electron densities of all

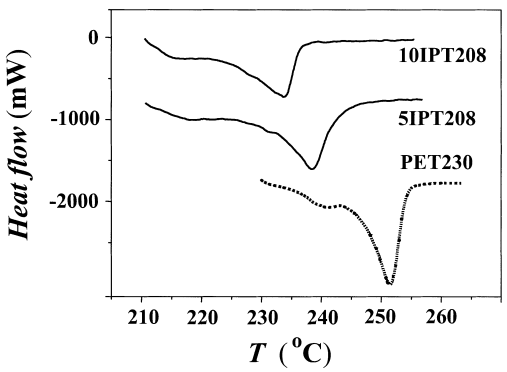

Fig. 7. DSC thermograms of PET and its copolymers (5IPT and 10IPT) measured during remelting after isothermal crystallization for 60 min at the chosen temperatures. The notation used indicates the polymer and its crystallization temperature: for example, PET230 refers to PET polymer crystallized at 230 °C. A heating rate of 3.0 K/min was employed.

the amorphous regions located in the interlamellar and interstack regions are the same. Therefore, Q in Eq. (4) is the invariant of the SAXS intensity profile for a sample composed of lamellar stacks with such ideally sharp interfaces.

In fact, a lamellar stack with ideally sharp interfaces is only a rough approximation to a real lamellar stack, in which all interfaces have a density gradient. However, Eq. (4) is a powerful practical tool for characterizing the density difference $(\rho_c - \rho_a)$ between the lamellar and amorphous layers in a crystallized sample which is composed of lamellar stacks. For each SAXS profile measured in this study, the invariant Q of the lamellar stacks with a sharp interface was thus estimated by extrapolating the linear fit of the first decay slope in the plot of $\gamma_1(z)$ versus z to $z = 0$, according to a method reported previously [38–40,48]. Some of the determined variations of Q with crystallization time are shown in Fig. 8. In the results presented here, the value of Q is normalized by its maximum value (Q_{max}) in order to clearly show its variation with crystallization time. As seen in Fig. 8, for PET the value of Q is small and constant for an initial induction period then increases rapidly with time up to a maximum at $t_{Q_{max}}$. Similar variations of Q with time are observed for the copolymers. In all cases the invariant Q reaches its maximum before $t = 60$ min.

Adopting Eq. (4), the $(\rho_c - \rho_a)$ term was estimated from the x_c and Q measured from samples isothermally crystallized for $t = 60$ min at the chosen temperatures. The $(\rho_c - \rho_a)$ terms estimated for each polymer system are plotted in Fig. 9 as a function of crystallization temperature T_c. Fig. 9 clearly shows that the electron density difference $(\rho_c - \rho_a)$ is larger in the copolymers than in the PET homopolymer over the range of T_c considered. This indicates that kinked IPT units in the copolymer are positioned mostly in the amorphous layer region rather than in the crystal region. The electron density difference also shows a tendency to become larger at higher values of T_c, regardless of polymer composition. This may result from the following two factors: first, slower crystallization at higher temperatures enables more effective exclusion of IPT units from the crystal region; second, the thermal expansivity is larger in the amorphous region than in the crystal region, and increasing the temperature may cause the thermal expansivity difference between the two regions to increase. Furthermore, the thermal expansivity difference may be larger in the copolymer than the homopolymer. This is evident in the d_c and d_a dependencies of T_c shown in Fig. 5.

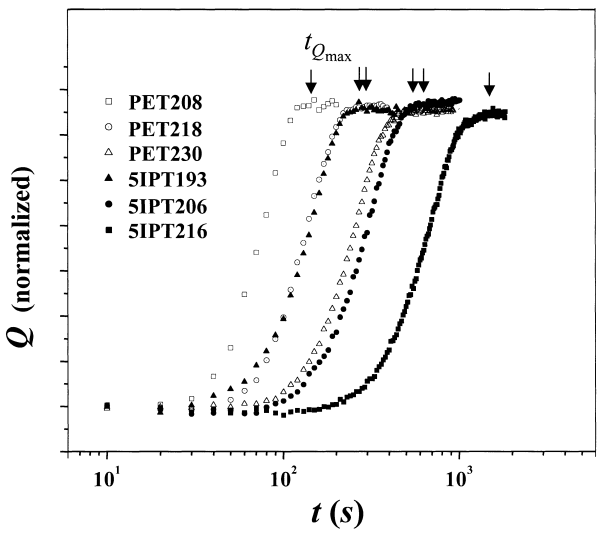

Fig. 8. Time dependence of the invariant Qs obtained from SAXS profiles measured during isothermal crystallizations of PET polymer and 5IPT copolymer at the chosen temperatures. For a sample being crystallized at a chosen temperature, the value of Q was normalized by its maximum value. The notation used indicates the polymer and its crystallization temperature: for example, PET230 refers to PET crystallized at 230 °C.

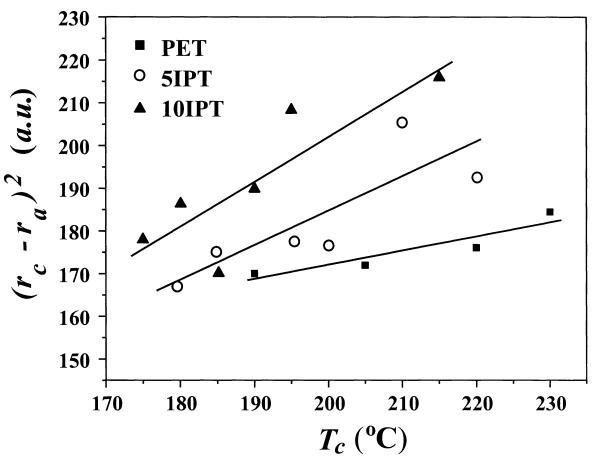

Fig. 9. Electron density difference between crystalline and amorphous regions calculated using Eq. (4) for PET homopolymer and its copolymers (5IPT and 10IPT). The values of x_c were measured by DSC from the samples isothermally crystallized for 60 min at the chosen temperatures.

4. Conclusion

The determination of morphological parameters, in particular the lamellar crystal and amorphous layer thicknesses (d_c and d_a) in crystallized PET polymer and its copolymers, was successfully carried out by one-dimensional correlation function analysis of the SAXS profiles measured during crystallization. The comprehensive analysis in this study clearly demonstrated that the one layer thickness l_1 derived from the correlation function analysis is the lamellar crystal thickness d_c rather than the amorphous layer thickness d_a in the lamellar stack. The d_c was found to be always smaller than d_a, regardless of polymer composition.

The crystal thickness d_c is highly dependent on the crystallization temperature, showing that the degree of supercooling is the major factor determining the thickness of lamellar crystals. d_c in PET is larger than in the copolymers, depending on crystallization conditions. However, no thickening occurs during the isothermal crystallizations, regardless of composition. Instead, the lamellar crystal undergoes perfectioning and lateral growth during the crystallization process, causing its melting temperature to shift to the high temperature region.

For the copolymers, the kinked isophthalate units are mostly excluded from the lamellar crystals into the amorphous layers during the crystallization process. This exclusion leads to an increase in the amorphous layer thickness; the values of d_a in the copolymers are larger than d_a in PET, depending on crystallization conditions. However, PET and copolymer systems crystallized at the same temperature form lamellar crystals with a similar thickness, although the copolymers are more likely to form thicker lamellar crystals due to their lesser degree of supercooling. This result might be due to the restriction of crystallization along the chain axis by the isophthalate units which have a kinked nature with some rigidity. The presence of isophthalate units lowers both the crystallization rate and crystallinity of the resultant polymer specimen.

In isothermal crystallizations the amorphous layer thickness d_a decreases with time, regardless of polymer composition. This decrease in d_a causes the reduction of the long period L during crystallization. The reasons for this decrease in d_a have been considered, taking into account several factors possibly influencing the crystallization process: (i) d_a distribution in lamellar stacks and its variation with time, (ii) the number of lamellae in lamellar stacks and its effect on SAXS profiles, and (iii) relaxation of polymer chains in the amorphous layers.

Acknowledgements

This study was supported by the Korean Ministry of Science and Technology (MOST) (KISTEP—Basic Research Grant of Nuclear Energy). The synchrotron SAXS measurements were supported by MOST and POSCO.

References

[1] Medellin-Rodriguez FJ, Phillips PJ, Lin JS. Macromolecules 1996;29:7491.
[2] Lee SW, Lee B, Ree M. Macromol Phys Chem 2000;201:453.
[3] Hauser G, Schmidtke J, Strobl G. Macromolecules 1998;31:6250.
[4] Wunderlich B. Polym Engng Sci 1978;18:431.
[5] Lin S-B, Koenig JL. J Polym Sci Polym: Polym Phys Ed 1983;21:2365.
[6] Kitano Y, Kinoshita Y, Ashida T. Polymer 1995;36:1947.
[7] Hachiboshi M, Fukuda T, Kobayashi SJ. Macromol Sci Phys 1969;3:525.
[8] Wang Z-G, Hsiao BS, Sauer BB, Kampert WG. Polymer 1999;40:4615.
[9] Holdsworth PJ, Turner-Jones A. Polymer 1971;12:195.
[10] Gedde UW. Polymer physics. London: Chapman & Hall; 1995. chapter 7.
[11] Fakirov S. Polymer 1980;21:373.
[12] Fakirov S, Seganov I, Kurdowa E. Makromol Chem 1981;182:185.
[13] Fakirov S, Seganov I, Prangowa I. Makromol Chem 1984;184:807.
[14] Seganov I, Schultz JM, Fakirov SJ. Appl Polym Sci 1986;32:3371.
[15] Lee SW, Ree M, Park CE, Jung YK, Park C-S, Jin YS, Bae DC. Polymer 1999;40:7137.
[16] Lee SW. MS Dissertation, Pohang University of Science and Technology Pohang, Republic of Korea; 1999.
[17] Yamadera R, Murano M. J Polym Sci: Part A-1 1967;5:2259.
[18] Jonas AM, Russell TP, Yoon DY. Colloid Polym Sci 1994;272:1344.
[19] Kruger K-N, Zachmann HG. Macromolecules 1993;26:1756.
[20] Fougnies C, Damman P, Vollers D, Dosiere M, Koch MHJ. Macromolecules 1997;30:1385.
[21] Zachmann HG. Nucl Instrum Methods Phys Res 1995;B97:209.
[22] Jonas AM, Russell TP, Yoon DY. Macromolecules 1995;28:8491.
[23] Wang W, Schultz JM, Hsiao BS. J Macromol Sci: Phys 1998;B37:667.
[24] Verma R, Marand H, Hsiao B. Macromolecules 1996;29:7767.
[25] Marand H, Alizadeh A, Farmer R, Desai R, Velikov V. Macromolecules 2000;33:3392.
[26] Wang J, Alvarez M, Zhang W, Wu Z, Li Y, Chu B. Macromolecules 1992;25:6943.
[27] Crist B, Claudio ES. Macromolecules 1999;32:8945.
[28] Alizadeh A, Richardson L, Xu J, McCartney S, Marand H, Cheung YW, Chum S. Macromolecules 1999;32:6221.
[29] Ikeda M. Chem Abstr 1968;69:19666.
[30] Lattimer MP, Hobbs JK, Hill MJ, Barham PJ. Polymer 1992;33:3971.
[31] Hsiao BS, Wang Z-G, Yeh F, Gao Y, Sheth KCZ. Polymer 1999;40:3515.
[32] Statton WO. J Appl Phys 1961;32:2332.
[33] Boyd RH. Polymer 1985;26:1123.
[34] Park B-J, Rah S-Y, Park Y-J, Lee K-B. Rev Sci Instrum 1995;66:1722.
[35] Bolze J, Kim J, Huang J-Y, Rah S, Youn HS, Lee B, Shin TJ, Ree M. Macromol Res 2002;10:2.
[36] Ruland W. J Appl Cryst 1971;4:70.
[37] Koberstein JT, Stein RS. J Polym Sci: Polym Phys Ed 1983;21:2181.
[38] Vonk CG, Kortleve G. Colloid Polym Sci 1967;220:19.
[39] Goderis B, Reynaers H, Koch MHJ, Mathot VBF. J Polym Sci: Phys Ed 1999;37:1715.
[40] Strobl GR, Schneider M. J Polym Sci: Polym Phys Ed 1980;18:1343.
[41] Scherrer P. Gottinger Nachrichten 1918;2:98.

[42] Klug HP, Alexander LE. X-ray diffraction procedures. New York: Wiley; 1954.
[43] Zachmann HG, Stuart HA. Makromol Chem 1960;41:148.
[44] Gehrke G, Riekel C, Zachmann HG. Polymer 1989;30:1582.
[45] Cebe P, Hong SD. Polymer 1986;27:1183.
[46] Vignaud R, Schultz JM. Polymer 1986;27:651.
[47] Choe CR, Lee KH. Polym Engng Sci 1988;29:801.
[48] Cruz CS, Stribeck N, Zachmann HG. Macromolecules 1991;24:5980.